

Effect of multiwalled carbon nanotube (MWNT) on the behavior of swelling of polyacrylamide–MWNT composites

Gülşen Akin Evingür¹ and Önder Pekcan²

Journal of Reinforced Plastics
and Composites

2014, Vol. 33(13) 1199–1206

© The Author(s) 2014

Reprints and permissions:

sagepub.co.uk/journalsPermissions.nav

DOI: 10.1177/0731684414526438

jrp.sagepub.com



Abstract

The purpose of this paper is to discuss the role of multiwalled carbon nanotube in the swelling of polyacrylamide–multiwalled carbon nanotube composites. Swelling experiments were performed in water at various temperatures by real-time monitoring of the decrease in pyranine (Py) and emission light intensity (I_{em}). The Stern–Volmer equation is modified for low-quenching efficiencies to interpret the behavior of pyranine intensity during the swelling of polyacrylamide–multiwalled carbon nanotube composites. The Li–Tanaka equation was used to determine the swelling time constants, τ , and cooperative diffusion coefficients, D , from fluorescence intensity, weight, and volume variations of the composite at various temperatures. It was observed that when τ decreased, naturally D increased by increasing temperatures.

Keywords

Polyacrylamide, multiwalled carbon nanotube, swelling, fluorescence, diffusion coefficient

Introduction

Carbon nanotubes (CNTs) were discovered in 1991. These materials have attracted enormous interest owing to their potential applications in field-emission devices, electronics, fibers, composites, sensors, detectors, capacitors, hydrogen storage media, and fuel cells, among others. The high mechanical strength makes them attractive materials for polymer reinforcement.^{1–2} Potential biological applications of both single walled (SWNT) and multiple wall (MWNT) carbon nanotubes have captured much imagination.³ Cyrille et al.⁴ carried the work about supramolecular self-assembly of lipid derivatives on CNTs.

Hydrogel is a hydrophilic three-dimensional network polymer; hence, it cannot dissolve when it holds a large amount of water and biochemical fluid. In order to keep the spatial structure, the polymer chains are usually physically or chemically cross-linked. Due to their swelling capacity, hydrogels can be easily rinsed to remove reagent residues. Hydrogels with better mechanical properties could be chosen through the penetration of interpenetrating polymer networks by chemical crosslinking. Therefore, the synthesis and

characterization of a composite gel with MWNT are studied by researchers.⁵ The behavior of composite laminates under structural and thermal loads was performed.⁶ Their electrical and thermal conductivities were improved. Epoxy laminates were prepared by using hybridization of glass fibers and MWNTs.⁷ Mechanical behaviors of the epoxy hybrid composites were characterized by using flexural, impact and fracture toughness tests; the kinetics of water absorption for the epoxy hybrid composites conformed to Fickian law behavior. The temperature and pH sensitivity, mechanical strength, and the response rates of the composites based on MWNTs and poly(*N,N*-diethylacrylamide-*co*-acrylic acid) hydrogels were studied. The results showed that the synthesized

¹Faculty of Science and Letters, Piri Reis University, Tuzla, İstanbul, Turkey

²Faculty of Science and Letters, Kadir Has University, Cibali, İstanbul, Turkey

Corresponding author:

Gülşen Akin Evingür, Department of Physics, Faculty of Science and Letters, Piri Reis University, 34940 Tuzla, İstanbul, Turkey.

Email: gulsen.evingur@pirireis.edu.tr

nanocomposites would be useful in medicine and pharmaceuticals.⁸ The swelling mechanism of hydrogel to induce solvatochromic shifting in single-walled carbon nanotubes (SWNT) near-infrared emission within a biocompatible hydrogel was studied.⁹ The preparation and characterization of polyacrylamide/MWNTs nanohybrid hydrogels with microporous structures were performed by Fourier transform infrared, scanning electron microscope, and transmission electron microscope.¹⁰

Our objective is to study the effect of MWNTs on the swelling process of the polyacrylamide (PAAm)–MWNT composites by using the steady-state fluorescence technique. The Stern–Volmer equation combined with Li–Tanaka equation explains the behavior of the swelling of the PAAm–MWNT composites at different temperatures. The swelling time constants, τ , and cooperative diffusion coefficients, D , were determined for the swelling of the composite prepared with various MWNT contents. Supporting gravimetric and volumetric swelling experiments were also performed by using similar gel samples. It was observed that τ decreased and naturally D increased by increasing temperature. Swelling energies, ΔE were measured and found to be strongly dependent on MWNT content in the composite gels. It is observed that ΔE values first increased up to 1% (wt) of MWNT, then decreased by increasing MWNT content, indicating that the different behaviors of the gel swelling exist in low and high conducting regions of the composite.

Experiment

Materials and methods

MWNTs were purchased from Cheap Tubes Inc., USA which was analyzed by the Delta Nu Advantage 532 Raman Spectrometer with 100–3400 wave number spectral range. Commercial MWNTs have an average inner diameter of 5–10 nm, outer diameter of 20–30 nm, density of approximately 2.1 g/cm³, and purity higher than 95% (wt).

Initially, the solution was prepared as follows: MWNTs were dispersed in the proportions of 10 parts MWNTs: 1–2 parts polyvinyl pyrrolidone: 2000 parts distilled water at 27°C. The required dispersion time is approximately 5 or 6 min with an interruption of 10 s, every 30 s at full or high amplitude by using ALEX ultrasonic equipment.

Composite was prepared by using 2 M Acrylamide (AAm, Merck) with various amounts (0.1–15% (wt)) of MWNTs stock concentration at 27°C.¹¹ Composite gels were formed by free radical copolymerization as follows: 0.71 g of AAm, 0.01 g of *N,N'*-methylenebisacrylamide (BIS, Merck), 0.008 g of ammonium persulfate

(APS, Merck), and 2 μ l of tetramethylethylenediamine (TEMED, Merck) were dissolved in 5 ml distilled water (pH 6.5). This was stirred (200 rpm) for 15 min to achieve a homogenous solution. All samples were deoxygenated by bubbling nitrogen for 10 min, each pre-composite gel solution of 5 ml was poured into a cylindrical glass tube and injector for drying and swelling experiments, respectively. After gelation was completed, the composites were cut into discs with 10 mm in diameter and 4 mm in thickness from the injector.

Gelation, drying, and swelling processes were performed by a Model LS-50 spectrometer of PerkinElmer, equipped with a temperature controller. Disc-shaped gel samples were placed on the wall of a 1 cm path length square quartz cell filled with water for the swelling experiments.

All measurements were made at 90° position, and spectral bandwidths were kept at 5 nm. We used Py in the PAAm–MWNT composites as a fluorescence probe. The Py is a derivative of pyrene including three SO₃[−] groups which can form bonds with positive charges on the gel. The Py can be attached to the gel by Coulombic attractions.

The composite was excited at 340 nm during in situ experiments, and emission light intensity, I_{em} , of the pyranine was monitored at 427 nm as a function of swelling time. As the water diffusion increased, I_{em} decreased and the scattered light intensity, I_{sc} , increased due to the increase in turbidity of the swelling gel.

At the same time, a gravimetric measurement was performed by measuring weight. The radius and thickness of the PAAm–MWNT composites were also measured to calculate the volume of the PAAm–MWNT composites from the formula for a cylinder's volume. The initial thickness is constant for all samples.

Results and discussion

Figure 1(a) and (b) presents the fluorescence spectra of pyranine from the PAAm–MWNT composites during the swelling process in pure water at 60°C for 1 and 10% (wt) MWNT at 80 min, respectively. In both cases, as the water uptake is increased, I_{em} decreased and I_{sc} increased. In order to elaborate the above findings, first it has to be mentioned that two different phenomena cause the decrease in the I_{em} ; first is the quenching of excited pyranines and the other is the scattering of light from the gel due to turbidity.

As far as the turbidity is concerned, it has been known that the swelling and elastic properties of acrylamide gels are strongly influenced by large-scale heterogeneities in the network structure.^{12,13} In the swollen state, these imperfections manifest themselves in a non-uniformity of polymer concentration. These large-scale concentration heterogeneities do not

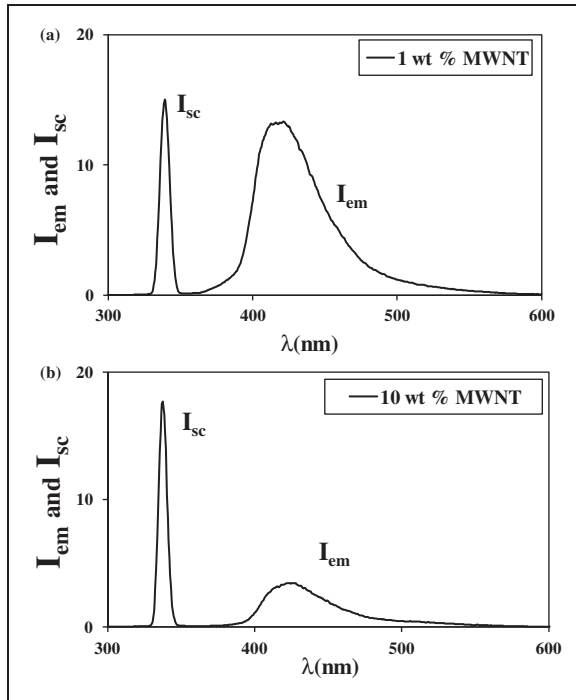


Figure 1. Fluorescence spectra of pyranine from the composite during swelling in water at 60°C for 1 and 10% (wt) MWNT content samples at 80 min.

appear in the dry state but only in the gel at the swollen, equilibrium state.¹⁴ Light scattering experiments by Bastide et al.¹⁵ seem to confirm this picture. When two junctions are located on neighboring lattice sites, a “frozen blob” is formed.¹⁷ In the swollen state of a gel, these cross-links cannot move apart from each other, since they are chemically connected by a chain segment which is in an optimal excluded volume conformation. Frozen blobs are often connected and form clusters of first topological neighbors. As a result, the random cross-linking of chains can be described as a site percolation on a blob lattice. When the gel is in a good solvent it swells and frozen blob clusters expand less than the interstitial medium. Here, the swelling of gel leads to an excess scattering of light which comes from the contrast between frozen blob clusters and holes created by the dilution. During the dilution process in gel swelling, the partial separation of frozen blob clusters leads to a strong increase of I_{sc} or decrease in the transmitted light intensity, I_{tr} .

In situ photon transmission technique for studying the aging of acrylamide gels due to multiple swelling was reported from our laboratory, where it was observed that the I_{tr} decreases continuously at the PAAm gel swells. The same technique was employed to study swelling of acrylamide gels with various cross linker concentrations, where decrease in I_{tr} was explained using the frozen blob model.¹⁶

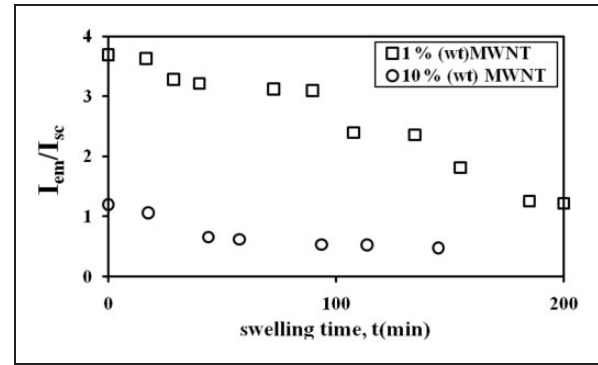


Figure 2. Corrected fluorescence intensities of pyranine, I ($=I_{em}/I_{sc}$) versus swelling time, t during the swelling process at 50°C for 1 and 10% (wt) MWNT content samples, respectively.

As far as the correction of I_{em} is concerned, totally empirical formula was introduced^{17–19} to produce the meaningful results for the fluorescence quenching mechanisms. Here, the main idea is to eliminate the structural fluctuation due to the frozen blobs and holes during swelling by using I_{sc} , i.e. one has to produce the corrected fluorescence intensity, I by dividing I_{em} to I_{sc} to exclude the effect of turbidity of the gel on the I_{em} and elaborate the Stern–Volmer model by using solely fluorescence intensity, I .

Figure 2 shows the variations of the corrected pyranine intensities, I ($=I_{em}/I_{sc}$) of the PAAm–MWNT composites versus swelling time during swelling process for 1 and 10% (wt) MWNTs contents at 50°C. As the swelling time, t , increased, quenching of excited pyranines increased due to water uptake.

In order to quantify these results, the collision type of quenching mechanism may be proposed for the fluorescence intensity, I , in the gel sample during the swelling process, where Stern–Volmer Model has been proposed²⁰

$$\frac{I_0}{I} = 1 + k_q \tau_0 [Q] \quad (1)$$

where k_q is quenching rate constant, τ_0 is the lifetime of the fluorescence probe, and Q is the quencher concentration. If one integrates equation (1) over the differential volume (dv) and for low quenching efficiency, ($\tau_0 k_q [Q] \ll 1$), of the gel from the initial, a_0 , to final, a_∞ , thickness, here water uptake, W , was calculated over differential volume by replacing Q with W and then reorganization of the relation produces the following useful equation

$$W = \left(1 - \frac{I}{I_0}\right) \frac{v}{k_q \tau_0} \quad (2)$$

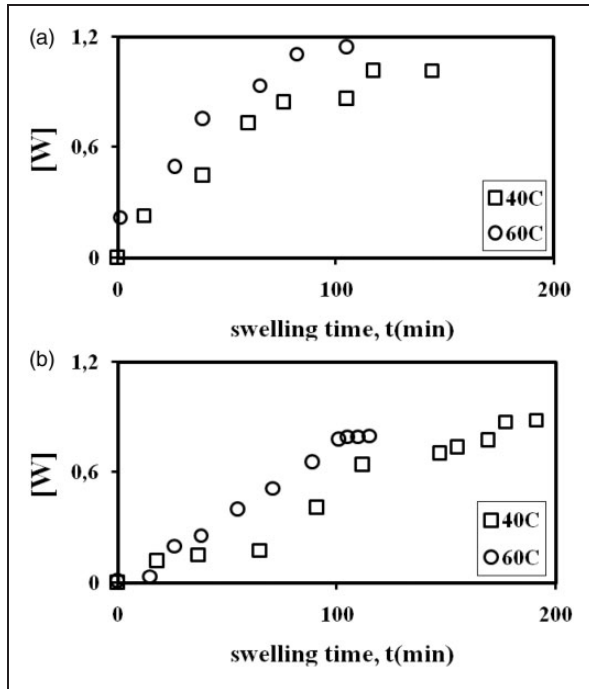


Figure 3. The plots of fluorescence data by using equation (2), versus swelling time, t , for PAAm–MWNT composite gels swollen in water measured by fluorescence technique for (a) 1 and (b) 15% (wt) MWNT content sample at 40°C and 60°C, respectively.

where v is the swollen volume of the gel at the equilibrium swelling, which can be measured experimentally. k_q was obtained from separate measurements by using equation (2) where the infinity equilibrium value of water uptake; W_f was used for each MWNT content. Since τ_0 was already known for the pyranine, measured values of v can be used to calculate k_q for each sample separately. Once the k_q values are measured, the water uptakes, W , can be calculated from the measured τ_0 values in each step of the swelling. Here, it is assumed that the k_q values do not vary during the swelling processes, i.e., the quenching process solely originates from the water molecules.

Plots of water uptake, W , versus swelling time are presented in Figure 3(a) and (b) for 1 and 15% (wt) MWNT content samples at 40°C and 60°C, respectively. These are typical solvent uptake curves, obeying the Li–Tanaka equation (3)^{21–23}

$$\frac{W}{W_f} = 1 - B_l \exp(-t/\tau_l) \quad (3)$$

The logarithmic form of the data was fitted to the following relation produced from equation (3)

$$\ln\left(1 - \frac{W}{W_f}\right) = \ln B_l - \frac{t}{\tau} \quad (4)$$

where τ is the time constant, measured by the fluorescence technique and B_l is related to the ratio of the shear modulus, μ and longitudinal osmotic modulus, M . Using equation (4), the linear regression of the curves in Figure 3 provided us with B_l and τ_l values. Taking into account the dependence of B_l on R , one obtains R values and from the α_1 - R dependence α_1 values was based on the method described by Li and Tanaka.²²

Then, using equation (5)

$$D = \frac{3a_f^2}{\tau_l \alpha_l^2} \quad (5)$$

cooperative diffusion coefficients D were determined for these disc-shaped composites and found to be around 10^{-9} m²/s. Experimentally obtained τ_l and D_l values are summarized in Table 1.

It should be noticed that D_l values increased by increasing temperatures, as is expected. On the other hand as seen in Table 1, at low-MWNT content region, D values increase up to 1% (wt) MWNT content for all samples under investigation indicating that water molecules can flow faster in the CNTs, which causes faster swelling of the composite gel. However, above 1% (wt) MWNT content D values start to decrease due to increasing the rigidity of the composite, where PAAm–MWNT composites become purely conducting material.¹¹ In other words, high conductivity due to high-MWNT contents results in low elasticity and slower swelling.

The plots of the solvent uptake, W , versus swelling time measured gravimetrically for two of the composites swollen in water are shown in Figure 4(a) and (b) for 1 and 15% (wt) MWNT content samples at 40°C and 60°C, respectively. These are typical solvent uptake curves, obeying the Li–Tanaka equation, equation (3). The logarithmic forms of the data in Figure 4 were fitted by using equation (4), from which B_l and the gravimetric time constant, τ_w were determined. Then, using equation (5), gravimetric cooperative diffusion coefficient D_w , was determined and is listed in Table 1 with the τ_w values. A similar behavior in D_w as for D_l was observed by increasing temperatures and MWNT contents.

The variations in the volume, V , of the PAAm–MWNT composites during the swelling process were also measured. The plots of the volume, V , versus swelling time for the PAAm–MWNT composites, swollen in water are presented in Figure 5, which are again typical solvent uptake curves, obeying the Li–Tanaka equation (3). The logarithmic forms of the data in Figure 5 were fitted by using equation (4) from which B_l and τ_v , volumetric time constants, were determined. Here, it is assumed that the relation between W and V

Table 1. Experimentally measured parameters of PAAm–MWNT composites for various temperature and MWNT content during swelling process.

% (wt) MWNT	T (°C)	τ_1 (min)	$D_1 \times 10^{-9}$ (m ² /s)	τ_{W} (min)	$D_{\text{W}} \times 10^{-9}$ (m ² /s)	τ_{V} (min)	$D_{\text{V}} \times 10^{-9}$ (m ² /s)
0	30	85	0.95	250	0.47	232.55	0.28
	40	48.5	4	73	0.5	189	0.35
	50	37.7	7.1	58	0.6	70	0.5
	60	25	7.3	47	1.2	47	0.85
0.3	30	58.82	0.6	77.51	0.72	90.9	0.86
	40	55	1.25	62	0.99	83.33	0.91
	50	35.71	1.73	55.55	1.11	58.82	1.07
	60	26.31	1.82	46.51	1.25	41.66	1.15
0.6	30	55	0.65	72	1.05	73	0.91
	40	50	1.7	50	1.25	62.11	1.05
	50	33.33	1.9	47.61	1.29	43.47	1.11
	60	25.64	2.5	40	1.8	37.03	1.89
1	30	48	1	69.44	1.18	69.44	0.99
	40	47.61	2.07	48.78	1.7	60.6	1.1
	50	32.25	2.44	37	1.8	38.46	1.26
	60	22.72	2.95	35.08	1.95	32.25	2.08
3	30	96	0.4	69.93	0.7	81.96	0.79
	40	95.23	0.44	58.82	0.71	76	0.89
	50	90.9	0.68	40.6	0.93	74.07	0.92
	60	83.33	0.76	35.35	1.48	52.63	1.08
5	30	98	0.38	70.92	0.63	95	0.7
	40	97	0.39	66.66	0.69	85.47	0.74
	50	95.23	0.59	45	0.48	78	0.76
	60	89	0.62	38.46	1.13	55.55	0.78
10	30	100	0.36	142.85	0.38	163.93	0.46
	40	98	0.37	69	0.41	90.9	0.57
	50	95	0.55	53	0.47	88	0.59
	60	91	0.6	45.45	0.58	58.82	0.61
15	30	120	0.32	150	0.27	238.09	0.37
	40	111.11	0.35	72.99	0.35	100	0.44
	50	105.26	0.44	64	0.43	83	0.48
	60	103.09	0.46	52.63	0.65	76.92	0.51

MWNT: multiwalled carbon nanotube.

was linear. The volumetric cooperative diffusion coefficients, D_{V} were produced by using equation (5) and are listed in Table 1 with the τ_{V} values.

The swelling time constants, τ , with respect to temperature measured by fluorescence, gravimetric, and volumetric techniques all present similar behaviors, i.e., gel swells faster as the temperature is increased during water uptake process. Minimum Li–Tanaka time constant has been observed at the highest temperature, where D values reached to their maximum values.

Temperature-dependent behavior of swelling, the composite predicts that D versus $1000/T$ relation obeys the following Arrhenius law

$$D = D_0 \exp(-\Delta E/kT) \quad (6)$$

where ΔE is the energy of swelling, k is Boltzmann's constant, and D_0 is the cooperative diffusion coefficients at $T = \infty$.

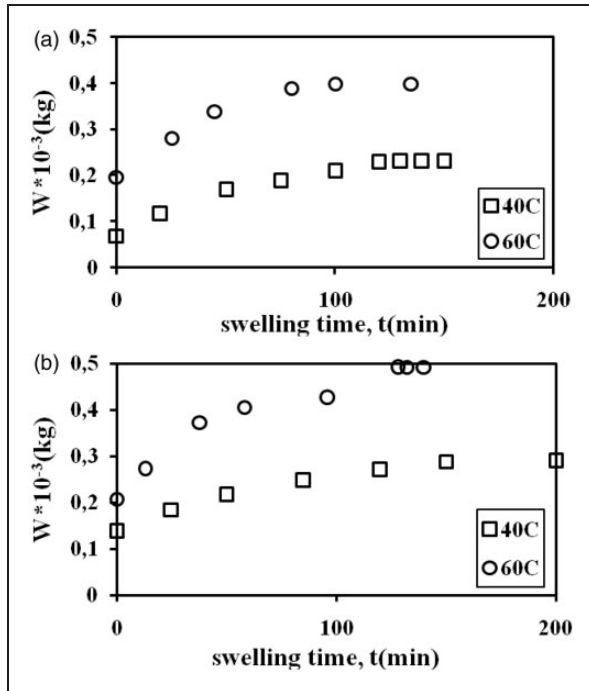


Figure 4. (a) The plots of the water release, W variation versus swelling time, t , for PAAM-NIPA composite gels swollen in water measured by gravimetric technique for (a) 1 and (b) 15% (wt) MWNT content samples at 40°C and 60°C, respectively.

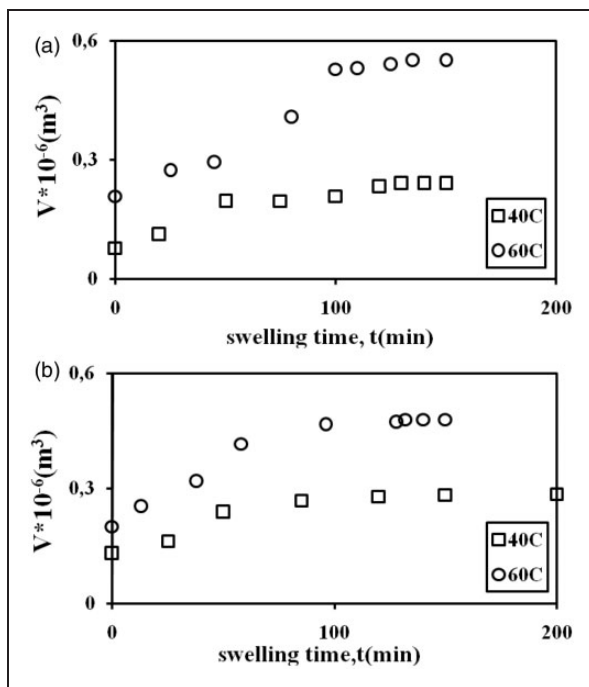


Figure 5. The plots of the volume, V , variation versus swelling time, t , for PAAM-MWNT composite gels swollen in water measured by volumetric technique at 40°C and 60°C for (a) 1 and (b) 15% (wt) MWNT content samples, respectively.

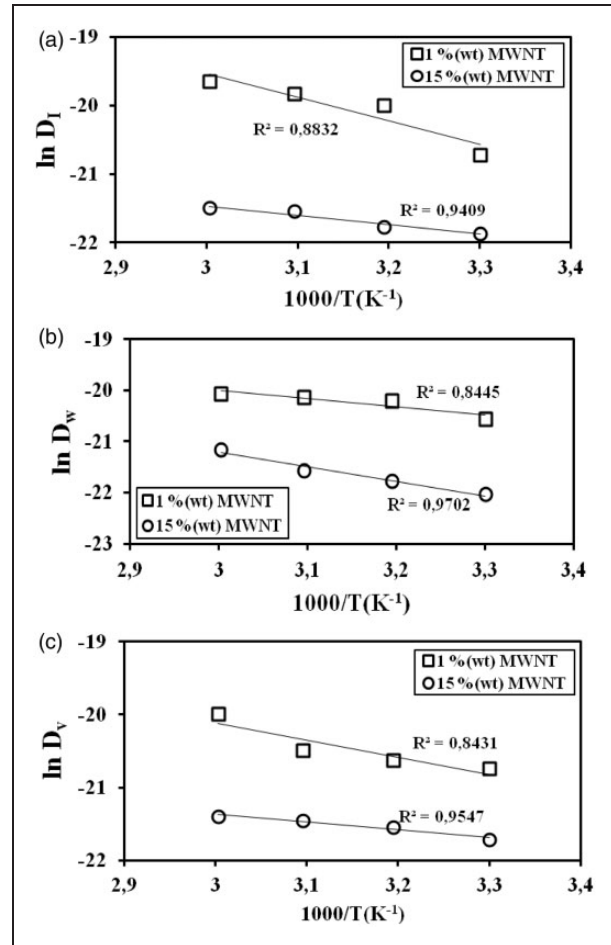


Figure 6. Linear regressions of diffusion coefficients versus reversed temperature measured by (a) fluorescence, (b) gravimetric, and (c) volumetric techniques for 1 and 15% (wt) MWNT content samples, respectively.

The logarithmic form of equation (6) is presented in Figure 6(a), (b), and (c) for the data obtained by fluorescence, gravimetric, and volumetric techniques, respectively, from which ΔE values are produced and listed in Table 2 and plotted versus % (wt) MWNT content in Figure 7(a), (b), and (c).

ΔE increased until 1% (wt) MWNT and then decreased. Above 5% (wt) MWNT, energy almost stays constant. Here, the behavior of ΔE versus % (wt) MWNT content is quite similar to the behavior of D . Below 1% (wt) MWNT, ΔE values increase by increasing MWNT content indicating that elastic system needs larger energy for swelling. However, above 1% (wt) MWNT due to high CNT content, network becomes less elastic so that swelling slows down at which the composite requires less energy for the swelling process. On the other hand, our previous experiments presented a study of the drying kinetics of PAAM-MWNT composite gels with various MWNT contents.²² It is also understood that the energy needed

Table 2. The measured energy during swelling for various % (wt) MWNT content gels by fluorescence, gravimetric, and volumetric techniques, respectively.

% (wt) MWNT	ΔE_f (kJ/mol)	ΔE_w (kJ/mol)	ΔE_v (kJ/mol)
0	34.2 ± 1.2	36.8 ± 1.1	43.2 ± 1.2
0.3	27.8 ± 1.3	13.2 ± 0.6	8.3 ± 0.9
0.6	29.9 ± 1.1	14.4 ± 0.7	17.9 ± 0.9
1	33.9 ± 1.3	20.1 ± 1.5	18.9 ± 1.2
3	19.1 ± 0.4	12.7 ± 0.9	7.8 ± 0.7
5	15.2 ± 1.3	10.8 ± 0.4	2.8 ± 0.8
10	15.6 ± 0.1	11.3 ± 0.5	7.2 ± 0.3
15	10.7 ± 0.5	12.9 ± 0.5	8.5 ± 0.4

MWNT: multiwalled carbon nanotube.

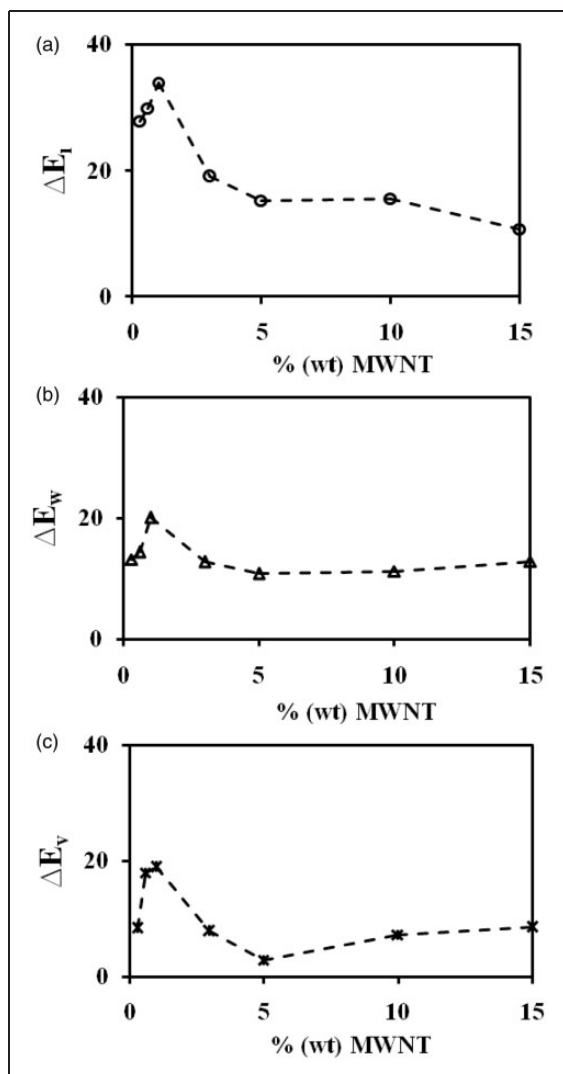


Figure 7. Energy versus wt (%) MWNT content measured by (a) fluorescence, (b) gravimetric, and (c) volumetric techniques, respectively.

for drying is different below and above the critical value of MWNT, at which the conducting percolation cluster starts to appear.¹¹ Below the critical value, composite gel is more elastic and the energy needed for drying decreases as the composite system reaches 1 wt % MWNT. At this point, the energy requirement for drying is minimal, due to the formation of percolation clusters from the CNTs, which helps the water molecules to run faster and exit from the composite gel system. However, above the critical point (1 wt % MWNT), the composite gel is quite stiff, due to the formation of an infinite network, which resists the shrinking process, and as a result, the system spends a larger amount of energy on the drying process at this region.

Conclusion

The results in this work have shown that the fluorescence method can be used to monitor the swelling kinetics of the PAAm–MWNT composites in water for various temperatures. This technique was employed to measure the swelling time constants, τ , and cooperative diffusion coefficients, D , for composite gels prepared with various PAAm and MWNT contents. The Li–Tanaka model was applied to measure these parameters. The results, here, were interpreted in terms of the swelling time constants, τ and the cooperative diffusion coefficient, D for all MWNT content gels. Here, basically composite assembly on the basis of intermolecular hydrogen bond or other non-covalent interactions was constructed in the presence of the MWNTs and PAAm networks, which further affected swelling performances of the composites. It is important to note that energy requirement of the swelling process is much less in the high-conducting, rigid region of the composite than in the low-conducting, more elastic region.

Acknowledgments

The authors thank Spectroscopy Laboratory in the Department of Physics Engineering, Istanbul Technical University for allowing them to carry out the experiments.

Funding

This research received no specific grant from any funding agency in the public, commercial, or not-for-profit sectors.

Conflict of interest

None declared.

References

- Satarkar NS, Johnson D, Marrs B, et al. Hydrogel-MWCNT nanocomposites: synthesis, characterization, and heating with radiofrequency fields. *J Appl Polym Sci* 2010; 117: 1813–1819.

2. Coleman JN, Khan U, Blau WJ, et al. Small but strong: a review of the mechanical properties of carbon nanotube–polymer composites. *Carbon* 2006; 44: 1624–1652.
3. Mattson MP, Haddon RC and Rao AM. Molecular functionalization of carbon nanotubes and use as substrates for neuronal growth. *J Mol Neurosci* 2000; 14: 175–182.
4. Cyrille R, Fabrice B, Patrick S, et al. Supramolecular self-assembly of lipid derivatives on carbon nanotubes. *Science* 2003; 300: 775–778.
5. Li H, Wang DQ, Chen HL, et al. Synthesis of a novel gelatin–carbon nanotubes hybrid hydrogel. *Colloids Surf B: Biointer* 2003; 33: 85–88.
6. McCrary-Dennis MCL and Okoli OI. A review of multi-scale composite manufacturing and challenges. *J Reinf Plast Compos* 2012; 31: 1687–1711.
7. Zulfhi NHM, Bakar AA and Chow WS. Mechanical and water absorption behaviors of carbon nanotube enforced epoxy/glass fiber composites. *J Reinf Plast Compos* 2013; 32: 1715–1721.
8. Liu H, Liu M, Zhang L, et al. Dual-stimuli sensitive composites based on multi-walled carbon nanotubes and poly(*N,N*-diethylacrylamide-co-acrylic acid) hydrogels. *Reac Func Polym* 2010; 70: 294–300.
9. Barone PW, Yoon H, Garcia RO, et al. Modulation of single walled carbon nanotube photoluminescence by hydrogel swelling. *ACS Nano* 2009; 3: 3869–3877.
10. Luo YL, Zhang CH, Chen YS, et al. Preparation and characterisation of polyacrylamide/MWNTs nanohybrid hydrogels with microporous structures. *Mat Res Innovations* 2009; 13: 18–27.
11. Aktaş DK, Evingür GA and Pekcan Ö. Critical exponents of gelation and conductivity in Polyacrylamide gels doped by multiwalled carbon nanotubes. *Compos Interfaces* 2010; 17: 301–318.
12. Dusek K and Prins W. Structure and elasticity of non-crystalline polymer networks. *Adv Polym Sci* 1969; 6: 1–102.
13. Silberger A and Kramer O. *Biological and synthetic networks*. Amsterdam: Elsevier, 1988.
14. Bastide J and Leibler L. Large-scale heterogeneties in randomly cross-linked networks. *Macromolecules* 1988; 21: 2647–2649.
15. Bastide J, Bove F and Busier M. *Molecular basis of polymer networks*. Berlin: Springer, 1989.
16. Pekcan Ö and Kara S. Photon transmission technique for monitoring swelling of acrylamide gels formed with various crosslinker contents. *Polymer* 2001; 42: 10045–10053.
17. Tanaka T and Fillmore DJ. Kinetics of swelling of gels. *J Chem Phys* 1979; 70: 1214–1219.
18. Li Y and Tanaka T. Kinetics of swelling and shrinking of gels. *J Chem Phys* 1990; 92: 1365–1372.
19. Zrinyi M, Rosta J and Horkay F. Studies on the swelling and shrinking kinetics of chemically crosslinked disk-shaped Poly(vinyl acetate) gels. *Macromolecules* 1993; 26: 3097–3102.
20. Evingür GA and Pekcan Ö. PAAM-kappa carrageenan (κ -car) composites: drying and swelling with various κ -car contents. *Acta Phys Polonica* 2012; 121: 169–171.
21. Evingür GA and Pekcan Ö. Monitoring of dynamical processes in PAAM-MWNTs composites by fluorescence method. *Adv Compos Mater* 2013; 21: 193–208.
22. Evingür GA and Pekcan Ö. PAAM-MWNTs composites: drying with various MWNTs contents. *J Polym Eng* 2012; 33: 33–39.
23. Birks JB. *Photophysics of aromatic molecules*. New York: Wiley, Interscience, 1971.